Taylor & Francis
Taylor & Francis Group

RESEARCH PAPER/REPORT

Dietary restriction increases protective gut bacteria to rescue lethal methotrexate-induced intestinal toxicity

Duozhuang Tang [a,b]*, Ting Zeng [a,c]*, Yiting Wang [a,b], Hui Cui [a,c], Jianying Wu [a,c], Bing Zou [a,c], Zhendong Tao [d], Liu Zhang [e], George B. Garside [f], and Si Tao [a,c]

aJiangxi Key Laboratory of Clinical and Translational Cancer Research, Department of Oncology, The Second Affiliated Hospital of Nanchang University, Jiangxi, China; bDepartment of Hematology, The Second Affiliated Hospital of Nanchang University, Jiangxi, China; cDepartment of Oncology, The Second Affiliated Hospital of Nanchang University, Jiangxi, China; dDepartment of Medical Laboratory Medicine, Jiangxi Province Hospital of Integrated Chinese & Western Medicine, Jiangxi, China; eIntensive Care Unit, Peking University People's Hospital, Beijing, China; fLeibniz Institute on Aging - Fritz Lipmann Institute (FLI), Jena, Germany

ABSTRACT

Methotrexate (MTX) is a typical chemotherapeutic drug that is widely used in the treatment of various malignant diseases as well as autoimmune diseases, with gastrointestinal toxicity being its most prominent complication which could have a significant effect on the prognosis of patients. Yet effective ways to alleviate such complications remains to be explored. Here we show that 30% dietary restriction (DR) for 2 weeks dramatically increased the survival rate of 2-month-old female mice after lethal-dose MTX exposure. DR significantly reduced intestinal inflammation, preserved the number of basal crypt PCNA-positive cells, and protected the function of intestinal stem cells (ISCs) after MTX treatment. Furthermore, ablating intestinal microbiota by broad-spectrum anti-biotics completely eliminated the protective effect achieved by DR. 16S rRNA gene deep-sequencing analysis revealed that short-term DR significantly increased the *Lactobacillus* genus, with *Lactobacillus rhamnosus GG* gavage partially mimicking the rescue effect of DR on the intestines of *ad libitum* fed mice exposed to lethal-dose MTX. Together, the current study reveals that DR could be a highly effective way to alleviate the lethal injury in the intestine after high-dose MTX treatment, which is functionally mediated by increasing the protective intestinal microbiota taxa in mice. Keywords: Dietary restriction, Methotrexate, Gut microbiota, Intestinal stem cells, intestinal toxicity

Introduction

The classic cytotoxic drug methotrexate (MTX) is a folic acid antagonist that inhibits cell growth and reproduction by inhibiting dihydrofolate reductase.[1–3] It is widely used for the treatment of acute leukemia and various solid tumors as well as autoimmune diseases, and is the gold standard drug for rheumatoid arthritis.[4–6] Unfortunately, MTX exhibits numerous side effects, involving gastrointestinal damage as well as bone marrow suppression.[7–10] When used at high doses, MTX antagonizes the synthesis of purines and interferes with DNA synthesis, which results in cell-cycle arrest during S-phase. Therefore, MTX application often targets rapidly dividing tumor cells as well as highly proliferative normal tissues, such as the intestinal epithelium.[2,11] A common gastrointestinal side effect of MTX, intestinal mucositis, often induces

symptoms such as diarrhea, infection, and bloody stools, which severely affects the life quality of patients and extends the treatment cycle.[12–15] Therefore, the resulting gastrointestinal toxicity is the main dose-limiting side effect of MTX application. However, efficient ways to alleviate the severe gastrointestinal side effects induced by MTX, especially at high doses, remains to be developed.

Intestinal epithelial cells as well as rapidly prolif-erating intestinal stem cells (ISCs) can be vastly depleted by the application of high-dose cytotoxic drugs, including MTX.[16,17] This is due to direct cell toxicity per se as well as intestinal damage caused by inflammation, leading to the destruction of the intestinal barrier, compromised digestion, and malabsorption, thus triggering a series of gastroin-testinal complications.[10,16,17] After the acute phase of

injury, the residual ISCs and a small number of progenitor cells reconstruct the ISC pool by self-renewal and proliferation; at the same time, they differentiate into intestinal epithelial functional cells such as enterocytes, enteroendocrine cells, Paneth cells, and goblet cells for the reconstruction of the intestinal epithelial system. Thus, ISCs are the driving force to maintain intestinal homeostasis as well as tissue regeneration after injury, and could serve as a potential key target to improve MTX-induced intestinal complications.[18–24]

Recently, it was reported that feeding mice with probiotics before and/or after lethal radiation combined with high-dose MTX treatment ameliorated destruction of villi and crypts, and extended the survival time of mice after treatment by a small extent.[16] However, the combined treatment still proved fatal for all groups. Another recent study showed that *Bacteroides fragilis* gavage reduced low-dose MTX-induced inflammation.[25] These studies suggest that microbiota could serve as a protective agent to reduce MTX-induced gut toxicity, but ways to manipulate the gut microbiota to achieve a more promising protective effect that can allow for the high-dose application of MTX remain to be explored. Additionally, it has been shown that 24 h-fasting could preserve ISC viability, as well as small intestine architecture and barrier function after high-dose etoposide[17] and that 4-week calorie restriction decreased intestinal toxicity induced by cyclophosphamide associated remodeling of gut microbiota.[26] Previously, we and others have shown that calorie restriction significantly decreases levels of inflammatory factors and enhances stem cell functionality.[27,28] However, whether calorie restriction can attenuate MTX-induced toxicity and the underlying mechanism has not been studied so far.

In the current study, we remarkably observed that mice pretreated with short-term DR (30% dietary restriction for 2 weeks) were fundamentally protected from lethal doses of MTX that otherwise kill *ad libitum* (AL)-fed mice. Intestinal mucositis induced by lethal-dose MTX was also significantly attenuated by DR. In particular, DR significantly protected basal crypt PCNA-positive cells from depletion by MTX, as well as preserved the functionality of ISCs in organoid formation and survival. However, ablating the gut microbiota with antibiotics completely eliminated the rescue effect by DR. Further analysis showed that DR significantly restructured intestinal flora with a prominent increase of *Lactobacillus*. Furthermore, gavage of AL-fed mice with *Lactobacillus rhamnosus* GG, which belongs to the Lactobacillales Order and has known protective effects on radio-/chemo- toxicity, partially mimicked the rescue effect achieved by DR. Of note, ablating the intestinal microbiota completely eliminated the rescue effect by DR, while gavage with a single probiotic was only able to partially recapitulate the strong protective effect by DR. Together, our study provides the first experimental evidence that DR protects ISC function and diminishes intestinal toxicity induced by lethal-dose MTX via a global regulation of gut microbiota, which if translatable could have great clinical implications regarding the dose-limiting application of MTX.

Results

DR remarkably increases survival rate of mice exposed to lethal doses of MTX

To study the effect of DR on mice exposed to lethal doses of MTX, mice were treated with 30% DR or fed with AL diet for 2 weeks before intraperitoneal MTX injection, with control groups injected with saline (Figure 1A). A high dose of MTX was used in the study to generate a high lethality injury to best see the protective effect by DR. Basal physiology before MTX administration was evaluated by measuring body weight, belly fat, and blood biochemical parameters. DR led to a gradual reduction of body weight within the first week after dietary intervention, which was then stable in the second week (Fig. S1A). Two-week DR also resulted in decreased belly fat, blood glucose concentration, triglycerides (TG), cholesterol (TC) and low-density lipoprotein (LDL), with an increased high-density lipoprotein (HDL) level observed (Fig. S1B, C). However, two-week DR had no significant impact on aspartate transaminase (AST) or alanine transaminase (ALT) (Fig. S1C). We examined the survival rate of AL and DR mice upon MTX treatment by setting up 3 independent experiments with a combined total of 45 mice per AL+MTX and DR+MTX groups, and with 10 mice per AL+Saline and DR+Saline groups. The results from all 3 independent experiments showed a high level of consistency which is why they were combined for analysis (Figure 1B). Strikingly, more than 80% AL mice died between day 3 and day 7
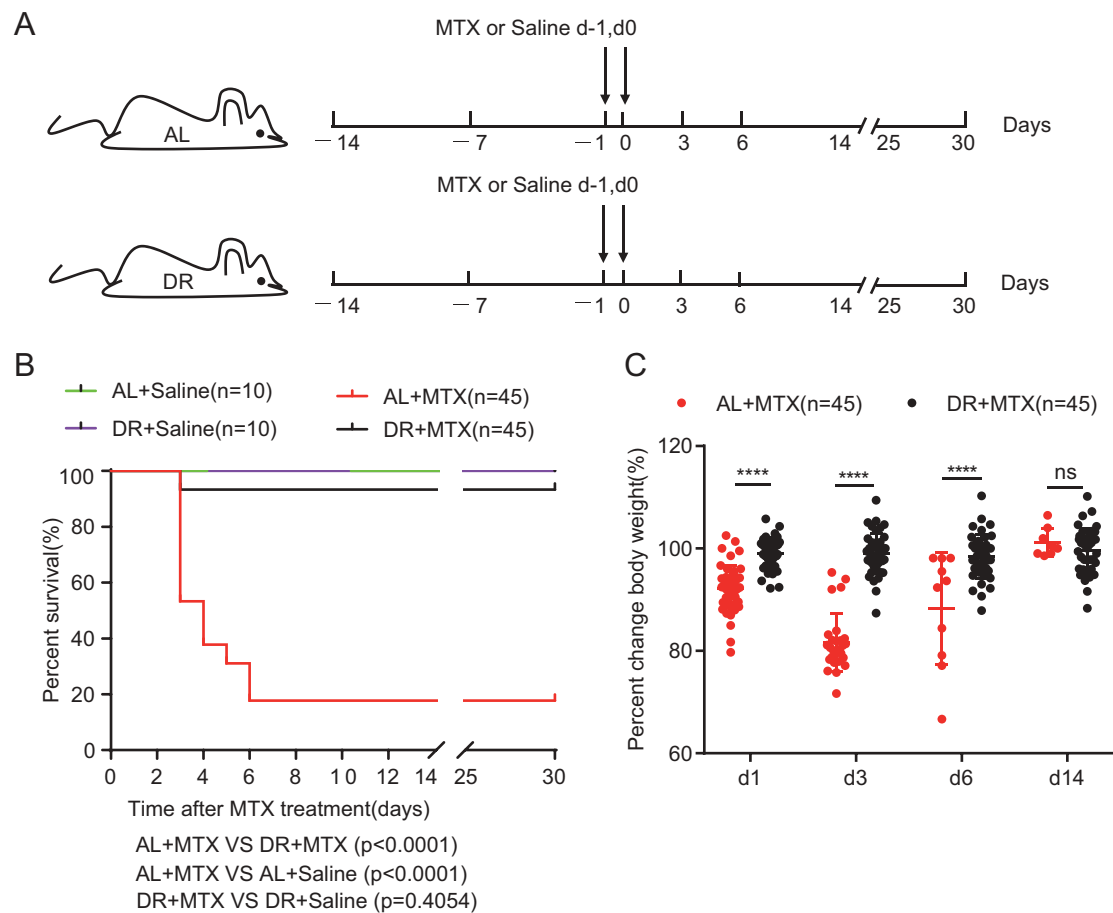
Figure 1. DR significantly improves survival rate and body weight maintenance of mice exposed to lethal doses of MTX treatment. (A) Scheme of experiment. Two-month-old mice were fed with AL diet or 30% DR diet for 14 days before MTX administration and the diet regimen was continued afterward. Then, mice were intraperitoneally injected with saline as control or MTX for 2 days at a dose of 120mg/kg (d-1) and 60mg/kg (d0). (B) Survival was monitored daily after MTX administration. (Data combined from 3 independent experiments. n = 45 mice per group for the AL+MTX mice and DR+MTX mice; n = 10 mice per group for the AL+Saline mice and DR+Saline mice) Gehan-Breslow-Wilcoxon test. (C) Percent change of body weight at indicated timepoints after MTX treatment compared to before MTX treatment (n = 45 mice per group, combined from 3 independent experiments). Note that the majority of mice were dead within 7 days after MTX administration, therefore, the number of mice measured in the AL group was much reduced at later timepoints after MTX treatment. Unpaired two-tailed, Student's t test. Results were displayed as mean±SD. n. s: nonsignificant; ****: $P < .0001$. AL: mice on AL diet; DR: mice on DR diet; AL+Saline: mice on AL diet and received saline injection; DR+Saline: mice on DR diet and received saline injection; AL+MTX: mice on AL diet and received MTX injection; DR+MTX: mice on DR diet and received MTX injection.

following MTX treatment, while more than 90% DR mice survived (Figure 1B). In the DR group, the survival rate was stable after day 3, while in the AL group, the survival rate continuously decreased until day 7 after MTX administration (Figure 1B). No further mice died up until the end of monitoring at day 30 (Figure 1B). Both AL+Saline and DR +Saline groups showed a 100% survival rate during the whole monitoring period (Figure 1B). In line with the survival rate, AL mice exhibited a remarkable reduction in body weight (Figure 1C).

On the contrary, body weight of DR mice after MTX treatment remained largely constant compared to their initial body weight before MTX injection, indicating a better overall health status (Figure 1C).

DR significantly protects small intestine and ISCs from lethal doses of MTX

To understand the mechanism underlying why DR maintained body weight and protected mice from death post MTX treatment, we first examined the

histology of the small intestines after MTX exposure. MTX-induced severe intestinal toxicity throughout the duodenum, jejunum, and ileum, as displayed by the great loss of villi and crypts, shortened villi, and decreased number of cells per crypt (Figure 2A–F). On the contrary, mice pre-treated with DR significantly maintained the height of villi, the number of crypts, and cell number per crypt (Figure 2A–F). In general, AL mice exhibited significant changes in the crypt-villus structure upon MTX treatment while the small intestine architecture of DR mice was much less affected and was essentially recovered by day 6 after treatment (Figure 2D–F). Of note, AL mice showed a strong reduction of villi height and crypt cell number on day 3 and a significant recovery on day 6 in the survived population, while DR mice maintained a relatively intact intestinal architecture (Figure 2D,F). These data suggest that DR strongly reduces intestinal toxicity caused by lethal-dose MTX and improves small intestine regeneration.

To further examine the effects of DR on the proliferative capacity of crypts, we counted the number of basal crypt PCNA-positive cells by immunofluorescent staining.[24,29] MTX administration resulted in a significant loss of basal crypt PCNA-positive cells in AL mice, with the strongest phenotype presenting on day 3 post-MTX treatment (Figure 2G,H). Intriguingly, the number of basal crypt PCNA-positive cells was significantly preserved by DR pre-treatment (Figure 2G,H). The formation of a crypt-villus axis in the standard 3D matrigel culture system reflects the proliferation capacity, as well as the differentiation activity of the plated ISCs.[30] To further explore the effect of DR on the functionality of injured ISCs, mice were treated with AL or 30% DR regimen for 2 weeks followed by MTX or saline intraperitoneal injection as described above (Figure 1A) and crypts of mice receiving different treatment were isolated on day 3 after MTX or saline injection and cultured. MTX treatment led to reduced seeding efficiency and impaired organoid formation in AL mice as shown by an increase in apoptotic organoids, whereas the growth of organoids from crypts derived from DR mice was significantly improved (seeding efficiency: 7.9 ± 4.6% in AL +MTX group versus 51.1 ± 19.7% in DR+MTX group; viable organoids per well: 1.8 ± 1.3 in AL +MTX group versus 79.4 ± 31.5 in DR+MTX group) (Figure 2I,J). Together, these data indicated that DR pre-treatment protected basal crypt PCNA-positive cells from depletion and preserved the functioning of ISCs after MTX administration, which could contribute to the improved regeneration under DR condition.

DR ameliorates MTX-induced intestinal inflammation

Previously we have shown that DR significantly inhibited expression of inflammatory factors in blood in undisturbed conditions.[27] DR was also shown to suppress inflammation in other models.[31,32] Since mucosal inflammation was considered to be the major cause of MTX-induced toxicity, we further examined the effect of DR on intestinal inflammation upon MTX administration. H&E staining shows that the small intestines of AL mice exhibited remarkable neutrophil infiltration and vascular congestion, associated with great loss of crypts and depletion of crypt cells, while intestines of DR mice presented minor signs of inflammation and relatively intact crypts (Figure 3A). The mucosal inflammation was further assessed by histology scores,[12] correspondingly, MTX treatment resulted in a notable elevation of the histology score in AL mice but not in DR mice (Figure 3B). In addition, immunofluorescent staining of CD11b+ myeloid cells showed much stronger inflammation induced in AL mice compared to DR mice (Figure 3C). To further examine the inflammatory activity, whole small intestine crypts were isolated to determine the expression of inflammation-related genes by qPCR analysis. MTX administration led to increased induction of inflammatory factors in AL mice, including IL-10, IL-1β, TNF-α, IFN-γ, and IL-6, whereas the induction was much less significant in DR mice (Figure 3D). These results indicated that high-dose MTX leads to a strong induction of mucosal inflammation in the intestine of AL mice while DR significantly suppressed it, which could play an important role in the general beneficial effect of DR on high-dose MTX-induced intestinal toxicity and mortality.
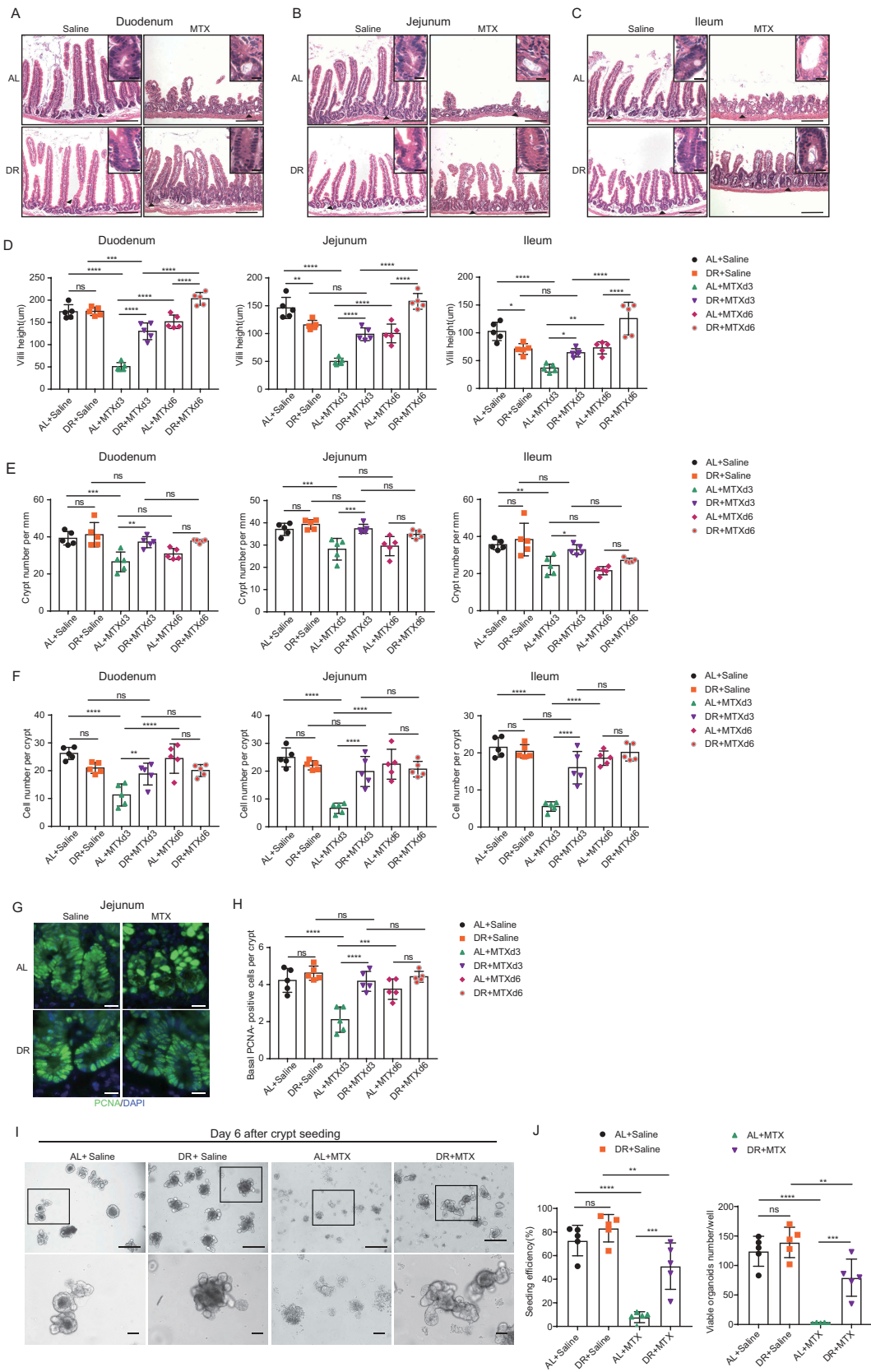
Figure 2. DR significantly protected small intestine and ISCs from lethal doses of MTX. Two-month-old mice were fed with AL diet or 30% DR diet for 14 days before MTX administration and the diet regimen was continued afterward. Then, mice were intraperitoneally injected with saline as control or MTX for 2 days at a dose of 120mg/kg (d-1) and 60mg/kg (d0). Mice were sacrificed at certain timepoints and small intestinal tissue was collected for further analysis. (A-C) Representative images of H&E staining of

## Ablating the gut microbiota eliminates the protective effects of DR

It was reported that supplementation of probiotics in rodents and human beings could reduce intestinal damage after radio- and/or chemotherapy.[16,25,33–36] To determine the role of intestinal microbiota in the DR induced protective effect under high-dose MTX administration, we applied broad-spectrum antibiotics (Abx) to DR pretreated mice to ablate the gut microbiota before MTX administration (Figure 4A). Remarkably, wiping out the microbiota completely diminished the beneficial effect on the overall survival rate achieved by DR (Figure 4B). Body weight on day 3 after MTX treatment revealed that ablating the microbiota also decreased the beneficial effect by DR on body weight maintenance (Figure 4C). To check the effect of removing gut microbiota on intestines, we analyzed intestinal histology by H&E staining. Antibiotic administration resulted in shortening of the villus height after MTX injection both under AL and DR conditions (Figure 4D,E). Crypt density was also reduced in the DR+Abx+MTX mice compared to the DR+Saline+MTX mice (Figure 4E). Further analysis of inflammation showed that the DR+Abx+MTX mice harbored similar levels of inflammation to the AL+Abx+MTX and AL+Saline+MTX mice, with the DR+Saline+MTX group significantly lower than all three other groups. Accordingly, the histological score of the DR+Saline+MTX group was around 5 times less compared to the other 3 groups (Figure 4E). In line with that, ablating the gut microbiota also significantly increased the CD11b labeled myeloid cell infiltration in intestines of DR mice (Figure 4F) and strongly up-regulated the expression level of inflammation genes in the crypts of DR mice,

including IL-10, IL-1β, TNF-α, and IFN-γ (Figure 4G). The number of basal crypt PCNA-positive cells was also significantly reduced in AL+Abx+MTX, AL+Saline+MTX, and DR+Abx+MTX groups compared to DR+Saline+MTX mice (Figure 4H,I). In the culture system, crypts derived from DR+Abx+MTX mice showed the impaired formation of organoids and increased death, which was similar to the culture of crypts from AL+Abx+MTX mice and AL+Saline+MTX mice, but distinct to the culture of crypts from DR+Saline+MTX mice. DR+Saline+MTX mice exhibited less death and better formation of organoids (seeding efficiency: 51.0 ± 7.2% in DR+Saline+MTX group versus 13.8 ± 6.6% in DR+Abx+MTX group; viable organoids per well: 75.2 ± 17.7 in DR+Saline+MTX group versus 8.2 ± 2.9 in DR+Abx+MTX group), suggesting that ablating the gut microbiota diminished the positive effect of DR on ISC maintenance and function upon MTX treatment (Figure 4J, K). Together, the results indicated that the protective effect of DR on lethal-dose MTX treated mice was mediated via the gut microbiota. In addition, since removing the intestinal flora diminished the positive effect of DR but had a minor impact on AL mice, we inferred that DR treatment might increase the abundance of bacterial taxa having protective potential against MTX treatment, rather than decreasing bacterial taxa that may induce intestinal damage upon MTX treatment.

DR modulates composition of intestinal flora

To investigate further, we analyzed the gut microbiota of AL and DR mice immediately before and 2 days after MTX injection (fecal samples on day 2

sections on day 3 after MTX administration (scale bar: 50μm). Square frames show the enlarged images of arrowhead pointed areas (scale bar: 20μm). (D) Villi height (30 crypts were counted for each mouse, n = 5 mice per group randomly picked from 2 independent experiments.) (E) Crypt number per millimeter (crypt number per 15 mm length was counted for each mouse, n = 5 mice per group randomly picked from 2 independent experiments.) and (F) cell number per crypt (30 crypts were counted for each mouse, n = 5 mice per group randomly picked from 2 independent experiments) at indicated timepoints after MTX administration. (G) Representative images of immunofluorescent staining of PCNA of jejunum on day 3 after MTX treatment (scale bar: 20μm). (H) Basal crypt PCNA-positive cell number per crypt counted from the whole small intestine at indicated timepoints after MTX administration (40 crypts were counted for each mouse, and n = 5 mice per group randomly picked from 2 independent experiments). (I) Representative images of cultured crypts on day 6 in culture derived from mice on day 3 after indicated treatment. Lower line: zoomed in vision of images in square frames of the upper line. Scale bars: 100 μm (upper); 50 μm (lower). (J) Seeding efficiency of cultured crypts on day 3 and number of viable organoids from cultured crypts on day 6 (n = 5 mice per group, combined from 2 independent experiments). Results were displayed as mean±SD. n.s: nonsignificant; *: $P < .05$; **: $P < .01$; ***: $P < .001$; ****: $P < .0001$ by One-way ANOVA test. AL+Saline: mice on AL diet and received saline injection; DR+Saline: mice on DR diet and received saline injection; AL+MTX: mice on AL diet and received MTX injection; DR+MTX: mice on DR diet and received MTX injection; d3: day 3 after MTX injection; d6: day 6 after MTX injection.
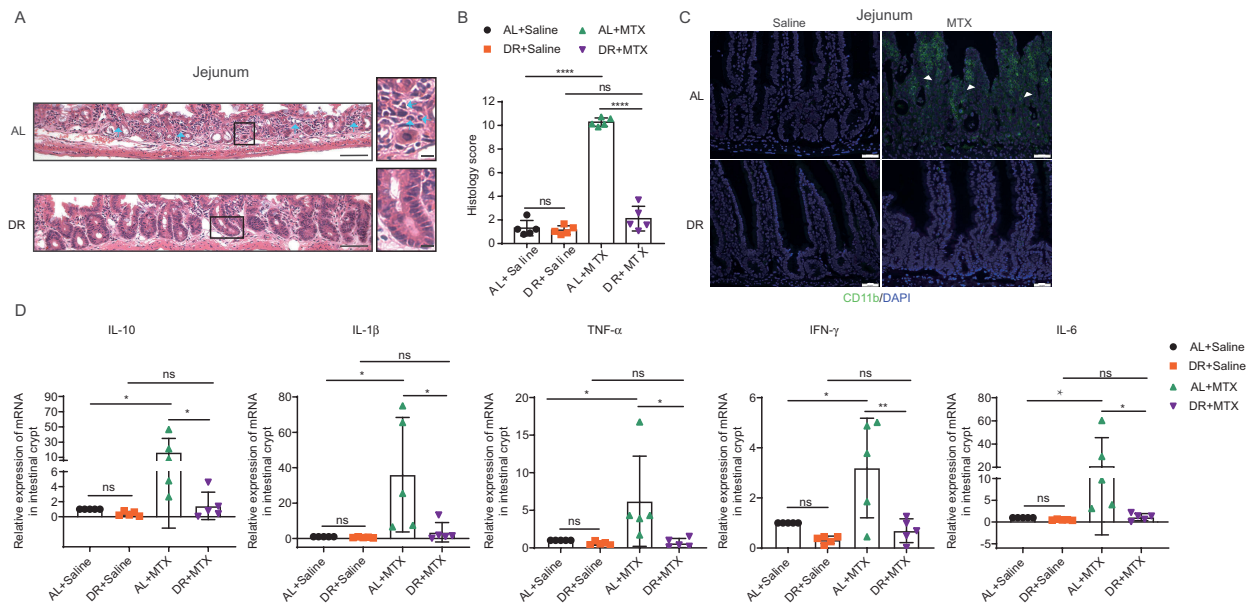
Figure 3. DR reduces MTX-induced intestinal inflammation. Two-month-old mice were fed with AL diet or 30% DR diet for 14 days before MTX administration and the diet regimen was continued afterward. Then, mice were intraperitoneally injected with saline as control or MTX for 2 days at a dose of 120mg/kg (d-1) and 60mg/kg (d0). Mice were sacrificed on day 3 after MTX administration and whole small intestinal tissue was collected for further analysis. (A) Representative images of H&E staining of jejunum. Representative crypts are shown in insets on the right. Note that crypts of DR mice were relatively intact while they were destroyed in AL mice with significantly increased neutrophils infiltration as pointed by blue arrows. Scale bar: 50µm (left), 20µm (right). (B) Histology score based on H&E staining. (33 vision fields were counted per mouse, n = 5 mice per group randomly picked from 2 independent experiments) of the whole small intestine. (C) Representative images of CD11b$^+$ immunofluorescent staining for myeloid cells of jejunum. Arrow heads point to CD11b$^+$ cells. Note the rare infiltration of CD11b$^+$ cells in DR mice compared to the extensive infiltration of CD11b$^+$ cells in AL mice after MTX administration. Scale bars: 20 µm. (D) Relative expression of indicated genes in freshly isolated crypt cells by qRT-PCR analysis (n = 5 mice per group randomly picked from 2 independent experiments). Results were displayed as mean±SD. n.s: nonsignificant; *: $P < .05$; **: $P < .01$; ***: $P < .001$; ****: $P < .0001$ by two-tailed, Student's t test. AL +Saline: mice on AL diet and received saline injection; DR+Saline: mice on DR diet and received saline injection; AL+MTX: mice on AL diet and received MTX injection; DR+MTX: mice on DR diet and received MTX injection.

after MTX injection was collected for analysis before the start of massive death in the AL group, and before heavy diarrhea hampered collection in this group) by 16S rRNA gene deep-sequencing (Illumina 250 bp paired-end). Interestingly, the overall structure of the gut microbiota was significantly shifted in DR treated mice compared to the AL mice, both before and after MTX injection, as shown by principal-coordinate analysis (PCoA) based on Bray–Curtis distance (Figure 5A). Of note, 2 weeks of DR treatment resulted in a significant shift in the composition of the gut microbiota at the level of Order (Figure 5B). Most prominently, short-term DR led to an increased relative abundance of the Order Lactobacillales in the intestinal flora (Figure 5B). We used the linear discriminant analysis (LDA) scores over 2 and looked at the top 9

bacteria in each direction (Figure 5C). The Order of Lactobacillales, Family of Lactobacillaceae and Genus of *Lactobacillus* were among the top 5 enriched taxa both before and after MTX administration (Figure 5C). In particular, the relative abundance of *Lactobacillus* was significantly increased both before and after MTX administration (Figure 5D). *Lactobacillus* is known to have protective potential on intestinal tissue exposed to radio- and/or chemotherapy, which might mediate the protective effect of DR on intestines exposed to lethal-dose MTX. To further examine the quantitative change of *Lactobacillus*, quantitative PCR (qPCR) was performed. The results show that amounts of total bacteria in the gut were not significantly altered (Figure 5E). Notably, DR significantly increased the detectable amount of *Lactobacillus* before as well as after MTX injection
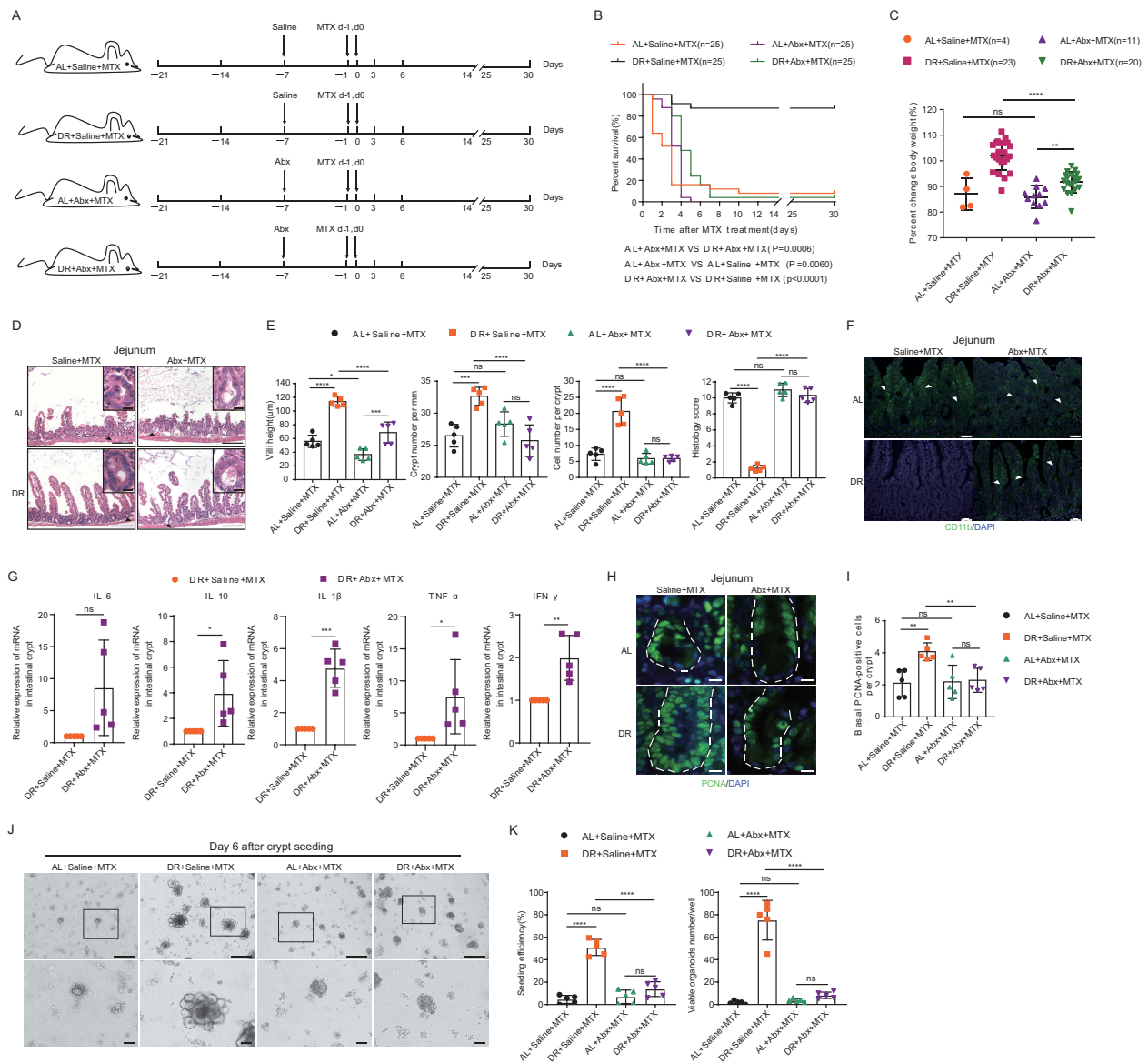
Figure 4. Ablating the gut microbiota eliminates the protective effect of DR. (A) Scheme of experiments. Two-month-old mice were fed with AL diet or 30% DR diet for 14 days before MTX administration and the diet regimen was continued afterward. Then, all mice were intraperitoneally injected with MTX for 2 days at a dose of 120mg/kg (d-1) and 60mg/kg (d0). Seven days prior to MTX administration, mice were fed by gavage for 5 days and then in drinking water for the following days with broad-spectrum antibiotics or saline. (B) Survival was monitored daily after MTX administration. Number of mice in each group was indicated. Gehan-Breslow-Wilcoxon test (n = 25 mice per group, combined from 2 independent experiments). (C) Percent change of body weight on day 3 after MTX treatment compared to before MTX treatment (number of mice of each group were indicated, results were from 2 combined independent experiments). Note that antibiotics treatment resulted in impaired body weight maintenance of DR mice. (D) Representative images of H&E staining of jejunum on day 3 after MTX administration. Representative crypts are shown in insets. Note that crypts of DR mice were relatively intact while they were destroyed in antibiotics treated mice after MTX administration. Scale bar: 50μm (outside), 20μm (insets). (E) Villi height (45 crypts were counted for each mouse, n = 5 mice per group randomly picked from 2 independent experiments), crypt number per millimeter (crypt number in 15 mm length as a unit was counted, and15 units were counted for each mouse, n = 5 mice per group randomly picked from 2 independent experiments), cell number per crypt (30 crypts were counted for each mouse, n = 5 mice per group randomly picked from 2 independent experiments) from the jejunum on day 3 after MTX administration were shown. Histology score was based on H&E staining (30 vision fields were counted per mouse, n = 5 mice per group randomly picked from 2 independent experiments) from the whole small intestine on day 3 after MTX administration. (F) Representative images of CD11b$^+$ immunofluorescent staining of jejunum on day 3 after MTX administration. Arrow heads point to CD11b$^+$ cells. Note antibiotics treatment induced the extensive infiltration of CD11b$^+$ cells in DR mice after MTX administration. Scale bars: 20 μm. (G) Relative expression of indicated genes in freshly isolated crypt cells from whole small intestine of mice on day 3 after MTX administration by qRT-PCR analysis (n = 5 mice per group randomly picked from 2 independent experiments). Note that antibiotics treatment significantly induced expression of inflammatory genes. (H) Representative images of

(Figure 5E). Together, these data indicated that DR increased the abundance of protective bacterial taxa in the gut.

We further examined alpha diversity to compare microbial richness and evenness in the broad-spectrum-antibiotics treated mice before and after MTX injection. As expected, the Shannon index decreased sharply in both AL and DR mice after antibiotics treatment, indicating that the structure of intestinal flora was heavily compromised by the broad-spectrum-antibiotics treatment in both AL and DR mice as shown by the alpha diversity analysis (Figure 6A). PCoA analysis showed that overall structure of AL and DR mice were significantly different before antibiotic treatment, but that difference disappeared after antibiotic treatment (Figure 6B). The relative abundance of *Lactobacillus* was similar among all groups after antibiotics treatment, regardless of whether the mice were treated with DR or MTX (Figure 6C). Coupled with that, the qPCR analysis showed a remarkable reduction in the amount of total bacteria as well as *Lactobacillus* upon antibiotic treatment in both AL and DR groups, with no significant difference among groups of mice treated with antibiotics (Figure 6D,E). These results indicated that bacterial richness, biodiversity, and the amount of *Lactobacillus* were severely compromised by broad-spectrum-antibiotics treatment in both AL and DR mice which negated the DR-mediated modulation of gut microbiota.

Lactobacillus rhamnosus GG gavage partially rescues survival of AL mice exposed to lethal doses of MTX

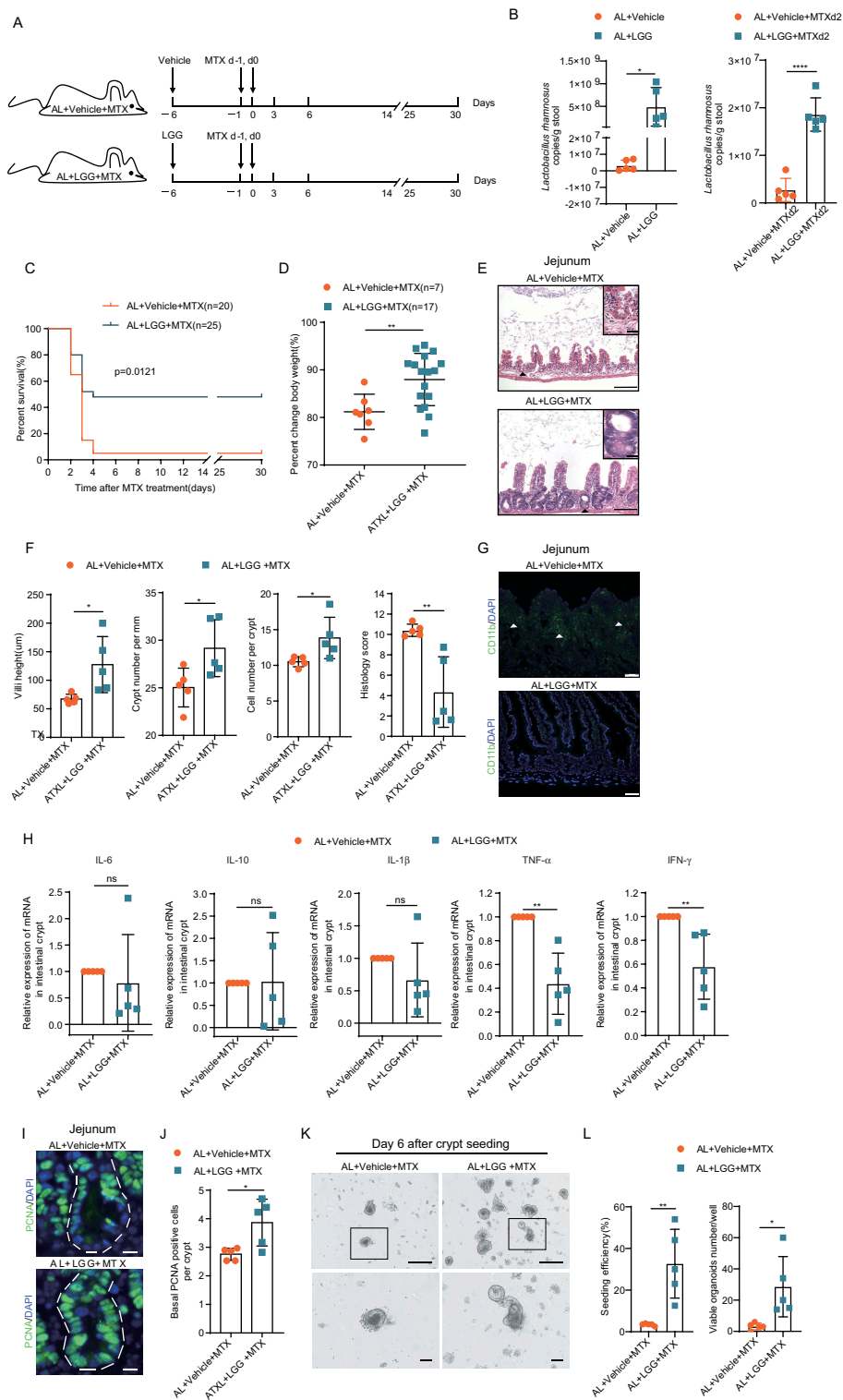To further investigate the relationship between the rescue effect of DR on high-dose MTX and its role in increasing beneficial bacterial taxa, we sought to mimic its rescue effect by gastric gavage of *Lactobacillus rhamnosus* GG (LGG). LGG was chosen as the *Lactobacillus* genus was found in higher abundance in DR both before and after MTX administration, as well as LGG belonging to the Lactobacillales lactic acid bacteria Order and being a well-known probiotic, known to protect against radio- and chemotherapy induced intestinal toxicities.[16,35,36] We applied LGG to AL mice for 5 days prior to the MTX administration (Figure 7A). qPCR analysis proved a significant increase in the amount of LGG in the LGG-fed mice both before and after MTX injection (Figure 7B). Interestingly, LGG gavage decreased the mortality rate to 52% on day 3 after which point a stable survival rate was maintained until the end of monitoring on day 30 (Figure 7C), and showed decreased body weight loss compared to the control group (Figure 7D). LGG gavage significantly improved intestinal architecture after MTX treatment, such as better maintenance of villi height, crypt density, and crypt cells, and histology score (Figure 7E,F). LGG gavage also diminished the infiltration of CD11b$^+$ myeloid cells and expression of inflammatory genes TNF-α and IFN-γ (Figure 7G,H). Furthermore, number of basal crypt PCNA-positive cells was also better maintained upon LGG-feeding in MTX injected AL mice (Figure 7I,J). LGG-feeding also significantly improved seeding efficiency and organoid formation of crypts from MTX treated AL mice comparing to vehicle-fed control mice (seeding efficiency: 3.4 ± 0.5% in AL+Vehicle+MTX group versus 32.7 ± 16.5% in AL+LGG+MTX group; viable organoids per well: 3.2 ± 2.2 in AL + Vehicle +MTX group versus 28.6 ± 19.3 in AL +LGG+MTX group) (Figure7K,L). These results indicated that supplementation of LGG can

immunofluorescent staining of PCNA of jejunum on day 3 after MTX treatment. (I) Basal crypt PCNA-positive cell number per crypt on day 3 after MTX administration of the whole small intestine (40 crypts were counted for each mouse, and n = 5 mice per group randomly picked from 2 independent experiments). (J) Representative images of cultured crypts on day 6 in culture derived from mice on day 3 after indicated treatment. Lower line: zoomed in vision of images in square frames of the upper line, note that antibiotics treatment diminished the protective effect in DR mice. Scale bars: 100 μm (upper); 50 μm (lower). (K) Seeding efficiency of cultured crypts on day 3 and number of viable organoids of cultured crypts on day 6 (n = 5 mice per group randomly picked from 2 independent experiments). Results were displayed as mean±SD. n.s; nonsignificant; *: $P < .05$; **: $P < .01$; ***: $P < .001$; ****: $P < .0001$ by one-way ANOVA. AL+Saline+MTX: mice on AL diet and received MTX injection and saline administration; DR+Saline+MTX: mice on DR diet and received MTX injection and saline administration; AL+Abx+MTX: mice on AL diet and received MTX injection and Abx administration; DR+Abx+MTX: mice on DR diet and received MTX injection and Abx administration.
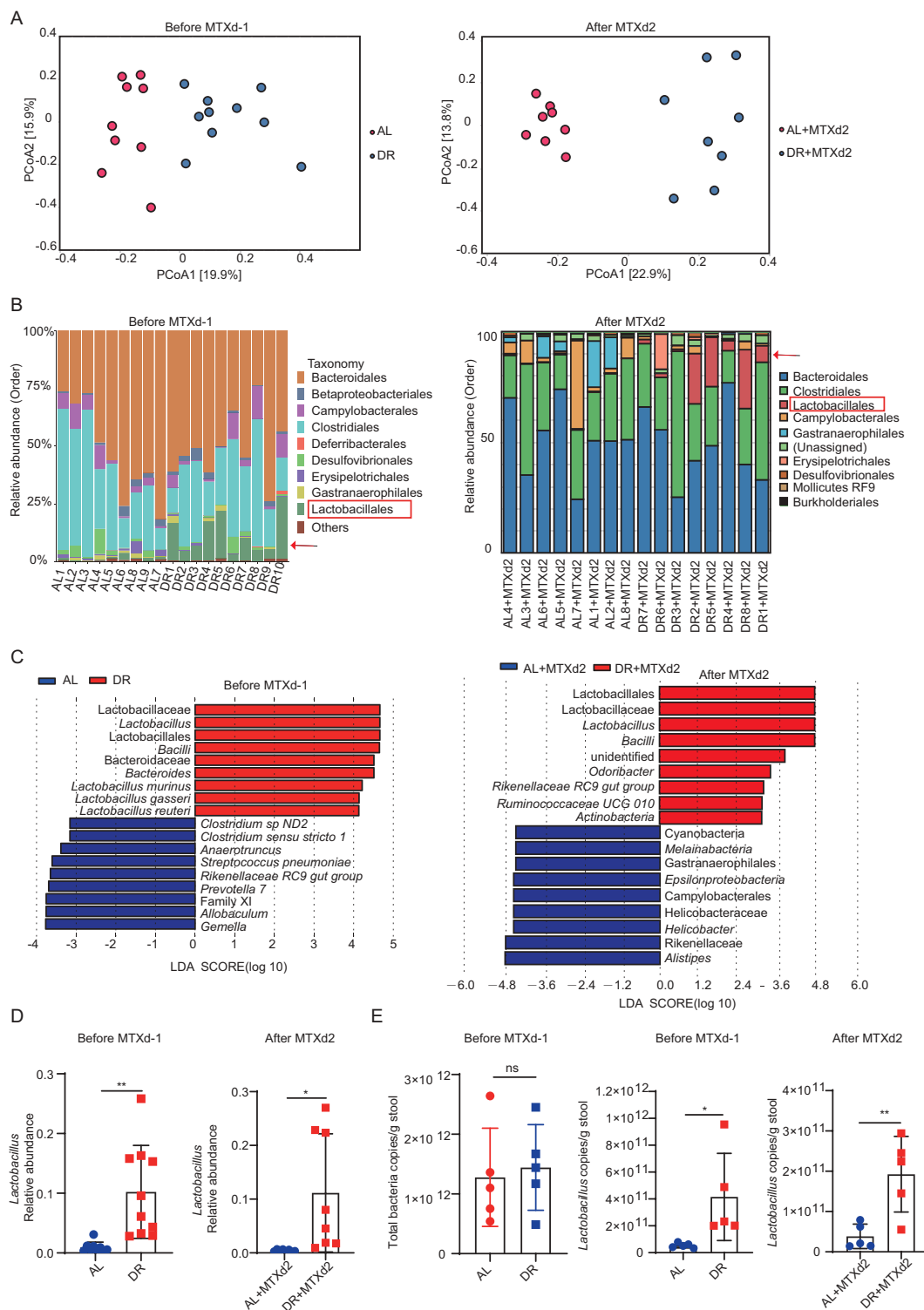
Figure 5. DR modulates composition of intestinal flora. Two-month-old mice were fed with AL diet or 30% DR diet for 14 days before MTX administration and the diet regimen was continued afterward. Then, mice were intraperitoneally injected with saline as control or MTX for 2 days at a dose of 120mg/kg (d-1) and 60mg/kg (d0) Fecal samples were randomly collected from mice before and on day 2 after MTX injection for 16S rRNA gene sequencing (n = 8–10 mice per group randomly picked from 2 independent experiments) and qPCR analysis (n = 5 mice per group randomly picked from 2 independent experiments). (A) Variation of intestinal flora structure of indicated groups along PC1 and PC2 of PCoA based on the Bray–Curtis distance. (B) Relative abundance of the intestinal flora of indicated groups on the Order level showed by 16S rRNA gene sequencing. (C) LDA scores in the fecal microbiomes of indicated groups. LDA score>2 and top nine bacteria were shown. (D) Relative abundance of the *Lactobacillus* showed by 16S rRNA gene sequencing. (E) qPCR analysis of the amounts of total bacteria and *Lactobacillus* of indicated groups (n = 5 mice per group, randomly picked from 2 independent experiments). Results were displayed as mean±SD. n.s; nonsignificant; *: $P < .05$; **: $P < .01$ by two-tailed, Student's t test. AL: mice on AL diet; DR: mice on DR diet; AL+MTX: mice on AL diet and received MTX injection; DR +MTX: mice on DR diet and received MTX injection; d-1: day −1 before MTX injection; d2: day 2 after MTX injection.

Figure 6. Broad-spectrum-antibiotics abolished differences of gut microbiota between AL and DR mice. Two-month-old mice were fed with AL diet or 30% DR diet for 14 days before MTX administration and the diet regimen was continued afterward. Then, all mice were intraperitoneally injected with MTX for 2 days at a dose of 120mg/kg (d-1) and 60mg/kg (d0). Seven days prior to MTX administration, mice were fed by gavage for 5 days and then in drinking water for the following days with broad-spectrum antibiotics or saline. Fecal samples were randomly collected from mice after 14 days on AL or DR diet before MTX injection and on day 2 after MTX injection for 16S rRNA gene sequencing (n = 5–8 mice per group randomly picked from 2 independent experiments) and qPCR analysis (n = 5 mice per group randomly picked from 2 independent experiments). (A) Shannon index of indicated groups based on alpha diversity analysis. (B) Variation of intestinal flora structure of indicated groups along PC1 and PC2 of PCoA based on the Bray–Curtis distance. (C) Relative abundance of the *Lactobacillus* showed by 16S rRNA gene sequencing. (D,E) qPCR analysis of the amounts of total bacteria (D) and *Lactobacillus* (E) of indicated groups (n = 5 mice per group, randomly picked from 2 independent experiments). Results were displayed as mean±SD. n.s; nonsignificant; *: $P < .05$; **: $P < .01$; ***: $P < .001$; ****: $P < .0001$ by one-way ANOVA. AL: mice on AL diet; DR: mice on DR diet; AL+Abx: mice on AL diet with Abx administration before MTX injection; DR+Abx: mice on DR diet with Abx administration before MTX injection; AL+Abx+MTX: mice on AL diet with Abx administration day 2 after MTX injection; DR+Abx+MTX: mice on DR diet with Abx administration day 2 after MTX injection.

Figure 7. LGG gavage partially rescued the survival of AL mice exposed to high-dose MTX. (A) Scheme of experiment. Two-month-old mice were fed with vehicle control or LGG for 5 days before MTX administration. Then, mice were intraperitoneally injected with the vehicle as control or MTX for 2 days at a dose of 120mg/kg (d-1) and 60mg/kg (d0). All mice were fed with AL diet. (B) qPCR analysis of the amounts of total bacteria and LGG of indicated groups (n = 5 mice per group randomly picked from 2 independent experiments). (C) Survival was monitored daily after MTX administration. Gehan-Breslow-Wilcoxon test. (n = 20–25 mice per group, combined from 2 independent experiments). (D) Percent change of body weight at indicated timepoints after MTX treatment compared to before MTX treatment (n = 7–17 mice per group, combined from 2 independent experiments). (E) Representative images of H&E staining of jejunum on day 3 after MTX administration. Representative crypts are shown in insets. Scale bar: 50μm (outside), 20μm (insets). (F) Villi height (40 crypts were counted for each mouse, n = 5 mice per group randomly picked from 2

partially mimic the rescue effect by DR upon MTX treatment. However, the rescue effect was less effective compared to DR, suggesting that a global modulation of the gut microbiota upon DR treatment plays an essential role in the protective mechanism of DR to MTX treatment.

Discussion

MTX is an established cytotoxic drug widely used in the treatment of malignant and autoimmune diseases. However, the strong intestinal toxicity induced by MTX is a major dose-limiting factor. As such, efficient ways to reduce the severe complications of MTX, which would allow for its high-dose application, would prove greatly beneficial. The current study provides the first experimental evidence in mice that short-term DR prior to high-dose MTX administration markedly reduced intestinal damage and increased survival rate compared to AL mice. In particular, DR preserved the viability as well as the regeneration functionality of ISCs exposed to high-dose MTX injury. Principally, we show that the beneficial effect achieved by DR was mediated by a global regulation of the intestinal flora and associated with a significant increase of the Order Lactobacillales. Our findings present DR as a novel way to ameliorate high-dose MTX-induced damage and provide insight into the underlying mechanism, which could be of great interest to clinicians as well as researchers aiming to reduce toxicity caused by dose-intensive chemotherapy.

Importantly, DR per se shows promising inhibition of spontaneous, chemically induced and radiation-induced tumors in multiple organs, including skin, breast, lung, liver, colon, pancreas, and prostate.[37] DR was also shown to restrict the growth and spread of cancer as well as sensitizing tumor cells to tumor treatment.[38–41] Therefore, it is tempting to speculate that DR treatment can markedly alleviate intestinal complications of MTX without disturbing its tumor killing effect, if not synergizing it.

Intestinal injury is a common complication of multiple chemotherapeutic drugs, and several studies have been conducted to find ways to ameliorate it. It was shown that 24-h fasting protected the structure and function of the small intestine in mice exposed to lethal doses of etoposide by activating DNA repair genes, faster resolution of DNA double strand breaks, reducing apoptosis in ISCs, and inhibition of infiltration of inflammatory cells.[17] However, the mechanism of how fasting achieved the above effects were not studied. A recent study showed that 4 weeks of calorie restriction prior to cyclophosphamide administration protected the intestinal barrier and epithelium, which was associated with a modulation of gut-microbiota.[26] Two other recent studies reported that probiotic supplementation ameliorated intestinal toxicity induced by a combination of lethal radiation and high-dose MTX treatment or low-dose MTX treatment alone.[16,25] These studies indicated an associated relation between intestinal flora and chemotherapy-induced intestinal damage.

The data presented here were generated using female C57BL/6J mice, so generalizability beyond this should be cautious given the microbiome variability introduced by sources such as the animal providers, rearing facilities, sex, and genetic background.[42,43] Previous studies have

independent experiments), crypt number per millimeter (crypt number in 15 mm length was counted as a unit, and 15 units were counted for each mouse, n = 5 mice per group randomly picked from 2 independent experiments), cell number per crypt (30 crypts were counted for each mouse, n = 5 mice per group randomly picked from 2 independent experiments) from jejunum on day 3 after MTX administration were shown. Histology score was based on H&E staining (30 vision fields were counted per mouse, n = 5 mice per group randomly picked from 2 independent experiments) from the whole small intestine on day 3 after MTX administration. (G) Representative images of CD11b$^+$ immunofluorescent staining of jejunum on day 3 after MTX administration. Arrow heads point to CD11b$^+$ cells. Scale bars: 20 μm. (H) Relative expression of indicated genes in freshly isolated crypt cells from the whole small intestine of mice on day 3 after MTX administration by qRT-PCR analysis (n = 5 mice per group randomly picked from 2 independent experiments). (I) Representative images of immunofluorescent staining of PCNA of jejunum on day 3 after MTX treatment. (J) Basal crypt PCNA-positive cell number per crypt of the whole small intestine on day 3 after MTX administration (30 crypts were counted for each mouse, and n = 5 mice per group randomly picked from 2 independent experiments). (K) Representative images of cultured crypts on day 6 in culture derived from mice on day 3 after indicated treatment. Lower line: zoomed in vision of images in square frames of the upper line. Scale bars: 100 μm (upper); 50 μm (lower). (L) Seeding efficiency of cultured crypts on day 3 and number of viable organoids of cultured crypts on day 6 (n = 5 mice per group randomly picked from 2 independent experiments). Results were displayed as mean±SD. n.s; nonsignificant; *: $P < .05$; **: $P < .01$; ***: $P < .001$; ****: $P < .0001$ by two-tailed, Student's t test.

highlighted, for example, the influence androgens can have on the gut microbiota.[44–46] Anatomical and microbiota differences between mice and humans, such as a relatively higher abundance of Lactobacillus in mice than humans,[47] may also impact on the translation of this finding to humans. Mouse models should never be viewed as a faithful equivalent to the human intestinal microbiota; however, these models allow for a detailed study of pathologies and functionalities on the hosts and therefore provide useful insights into the direct effects on intestinal tissue. Moreover, a small proportion of AL mice survived the high-dose MTX treatment and the survival rate stabilized after day 7. The underlying mechanism could be related to individual variations on drug metabolism, etc., and regeneration of the intestinal epithelium driven by ISCs in the survived mice, which was not deeply explored in the current study.

Previous studies have uncovered changes in intestinal microbiota upon chemotherapy-induced inflammation, and differentiating whether the change is causative or consequential has been very difficult.[48] Nevertheless, it has been shown that abrogating intestinal microbiota by broad-spectrum antibiotics resulted in enhanced inflammatory signatures, including substantial increases in inflammatory signaling and activation of dendritic cells.[49] In line with this, our study showed an even higher mortality rate in AL mice after broad-spectrum antibiotic treatment, which suggests that recent Abx application probably increases intestinal toxicities of MTX treatments. Furthermore, a wealth of studies has shown that gut microbiota modulates the actions of chemotherapeutic drugs through multiple mechanisms, including translocation, immunomodulation, metabolism, enzymatic degradation, and reduced diversity and ecological variation.[50] Therefore, it is believed that the gut microbiota can be targeted to improve efficacy and reduce the toxicity of chemotherapy agents.[26,50,51] In this regard, Abx application might also interfere with the MTX tumor killing capacity. Overall, one should be cautious in using Abx prior to or in combination with chemotherapy.

MTX administration has previously been shown to induce inflammation in mice, as well as reduce the diversity of the gut microbiota, and change macrophage M1/M2 polarization.[25] The observed decrease in intestinal inflammation caused by DR may be additionally mediated by changes in immune cell cytokine secretion,[52] as well as changes in the amount and/or type of bioactive metabolites secreted by the changed microbial composition.[53] Multiple studies have proved that the application of probiotics can attenuate abnormalities of inflammatory cells induced by chemotherapies.[34,54,55] In line with that, our study revealed that DR attenuated the infiltration of CD11b+ cells. It is possible that DR-mediated modulation of gut microbiota ameliorates changes in inflammatory cells upon MTX treatment, which requires further future investigation.

Our study shows that DR attenuated MTX-induced intestinal damage, accompanied by a global up-regulation of "protective" bacterial taxa, whose protective effect could be eliminated through antibiotic treatment or partially mimicked by LGG gavage. Therefore, the current study provided the first experimental evidence that under chemotherapy treatment DR preserved proliferative capacity of crypt cells and ISC function, accompanied with reduced intestinal toxicity via global modulation of gut microbiota. Furthermore, though a variety of chemotherapeutic agents can induce intestinal toxicity, the damaging level to the intestine specifically can be quite different at clinical doses. In the clinic, for cyclophosphamide the major complications are hemocytopenia and hemorrhagic cystitis,[56,57] and likewise with etoposide mainly hemocytopenia.[58,59] However, the predominant side effect of MTX is severe intestinal mucitis,[10,12,60] which can be sometimes lethal, especially at high doses. The intestinal toxicity is the major dose-limiting factor of MTX administration. The current study presents a novel way to eliminate the intestinal damage induced by high-dose MTX, and explores the underlying mechanism, which could be of great interest to the clinical applications of MTX.

Materials and methods

Mice and dietary intervention

Mice were bought from Beijing Speyford Laboratory Animals and maintained in the animal facilities of Nanchang Royo Biotech. Two-month-old C57BL/6J

female mice were maintained a 12-h light/dark cycle in the feeding environment under SPF-level feeding conditions. Mice were housed individually and received a regimen of either an AL diet (fed with an unlimited amount of food) or a DR diet (fed daily with an amount of food corresponding to 70% of the amount of food consumed by body weight – and gender-matched mice in the AL group). The provided food amount was constant over the whole DR period.[27] All mouse experiments were approved by the Animal Experimental Ethical Inspection of Nanchang Royo Biotech Co. Ltd (RYEI20170507-1).

MTX treatment

Protocol of MTX administration was modified from a previous publication.[10] Mice were given intraperitoneal injection of MTX (LingNan Pharmacy) at a dose of 120 mg/kg on day −1 and 60 mg/kg on day 0. The survival status and the body weight of the mice were monitored daily. A euthanasia criterion of 25% weight loss was followed for all mice.

Antibiotic treatment

Mice were fed by way of gavage with 0.2 ml broad-spectrum antibiotics at a concentration of 10 mg/mice/day including ampicillin (Solarbio), neomycin (Solarbio), metronidazole (Solarbio) and vancomycin (Lilly, Inc.) for 5 days, then the antibiotics were administered in drinking water (ampicillin, neomycin, and metronidazole: 1 g/L; vancomycin: 500mg/L) until the end of the experiment. Drinking water was exchanged twice a week. For the control group, saline was administrated in the same way as the antibiotics.

Fecal sample collection

Fresh fecal pellets were directly collected from each mouse in 1.5 ml microtubes by positioning the microtube in the proximity of the anus of the mouse and collect the pellets that are excreted. All samples stored at −80°C within 1h until DNA isolation for 16S rRNA gene sequencing.

Fecal DNA isolation

Fecal samples were weighed and total DNA was extracted with the DP328 Fecal Genome Extraction Kit (Tiangen Biotech) according to the manufacturer's instructions. DNA concentration and purity were measured with Nanodrop 2000.

Histology

Intestinal cross-sections through intestinal rolls spanning the entire small intestine were prepared as previously described.[61] Three-micrometer paraffin sections of the intestines were used for H&E staining. Five-micrometer paraffin sections of the intestines were used for immunofluorescent staining. Antibodies used were the following: PCNA (Abcam, ab29) 1:500 diluted; CD11b (Peprotech, 101204) 1:500 diluted; DAPI-containing sealing tablet (Solarbio).

All the images were taken by using the OLYMPUS IX73 microscope. The length of villi height and crypt number per millimeter were taken by using CELLSENS. The histology score ranged from 0 to 13 and was subdivided in the following categories: villus aspect (0 = normal,1 = short, 2 = extremely short), villus tops (0 = normal, 1 = damaged, 2 = severely damaged), epithelium (0 = normal, 1 = flattened, 2 = damaged, 3 = severely damaged), inflammation (0 = no infiltration, 1 = mild infiltration, 2 = severe infiltration), crypts (0 = normal, 1 = mild crypt loss, 2 = severe crypt loss), crypt abscesses (0 = none, 1 = present) and bleeding (0 = none, 1 = present).[12] Histology scoring and PCNA counting were based on the analysis of the whole small intestine with representative images from the jejunum shown. Villi height, crypt number per mm, and cell number per crypt were analyzed as duodenum, jejunum, and ileum separately. Results for Villi height, crypt number per mm, and cell number per crypt from different intestinal sites are shown in Figure 2, whereas only jejunum results were shown in Figures 4 and 7.

Crypt culture

Crypt culture was performed as previously described.[62] Briefly, isolated crypts were resuspended in cold matrigel (BD) containing Y27632 (Abcam), hR-spondin-1(PeproTech), mEGF (PeproTech),

hNoggin (PeproTech), CHIR99021(Tocris), and penicillin/streptomycin, and plated in 24-well plates in triplicates for each sample at a density of 200 crypts per well. Four hundred microliters of advanced DMEM/F12 medium (Invitrogen) containing B27 (Invitrogen), N2 supplement (Invitrogen) and 1.25 mM N-acetylcysteine were added to each well to cover the matrigel. In the culture system final concentrations of the following components were hRspondin-1 1 μg/ml, mEGF 50 ng/ml, hNoggin 100 ng/ml, CHIR99021 10mM and Y27632 10 μM. The medium containing growth factors was changed every 3 days.

RNA isolation and cDNA synthesis

Total RNA was isolated from fresh crypts by using RNApure Tissue Kit (CWbiotech) following the manufacturer's instructions. Reverse transcriptions were performed to synthesize first strand DNA by using TransScript-Uni One-Step gDNA Removal and cDNA Synthesis SuperMix kit (TransGen Biotech) according to the manufacturer's instructions with a procedure of incubation at 42°C for 15 min and heating inactivation at 85°C for 5 s.

Quantitative Real-Time PCR (qPCR)

For intestinal crypt samples, qRT-PCR was performed using TransStart Tip Green qPCR SuperMix (TransGen Biotech) with an ABI 7900 Real-Time PCR system (Applied Biosystems) in triplicates. The reactions were performed under the following conditions: 94°C for 30 s, 40 cycles of 94°C for 30 s followed by 60°C for 30 s. mRNA expression of genes was normalized to β-actin in each sample and was normalized to 1 in the AL group and AL+Saline+MTX group. Primer sets for the detection of single genes were either self-designed (IL-6) or taken from literature as follows β-actin from Tang et al.,[27] IL-1β from Seo et al.,[63] IFN-γ from Bamias et al.,[64] TNF-α and IL-10 from Sassone-Corsi et al.[65] Primer sequences were listed in Supplementary Table S1.

For fecal samples, qPCR assays were carried out using Ace qPCR SYBR Green Master Mix kit (Vazyme) with Bio-RAD 9600A system following the manufacturer's instructions. The reactions were performed under the following conditions:

94°C for 5 min, 40 cycles of 94°C for 15 s followed by 60°C for 30 s and 72°C for 30 s. The copy number of target DNA was determined by serially diluting standards (10^4 to 10^8 copies of plasmid DNA containing the respective amplicon for each set of primers) running on the same plate. The bacterial quantity was expressed as copies per gram of stool. Primer sets for the detection of bacteria taxa were picked from previous publications[66-69] and were listed in Supplementary Table S2.

16S rRNA gene sequencing

Fecal-sample DNA was extracted using DNA extraction kit (Minkagene Stool DNA kit), and 16S rRNA gene regions V3-V4 were amplified using universal primers[70] (338F 5′-ACTCCTACGGGAGGCAGCAG -3′ and 806R 5′-GGACTACCAGGGTATCTAAT-3′) with 12 bp barcode, PCR reactions, containing 25 μl 2x Premix Taq (Takara Biotechnology, Dalian Co. Ltd., China), 1 μl each primer (10 M) and 3 μl DNA (20 ng/μl) template in a volume of 50 μl.

The length and concentration of the PCR product were detected by 1% agarose gel electrophoresis. PCR products were mixed in equimolar ratios according to the GeneTools Analysis Software (Version4.03.05.0, SynGene). Then, the PCR mixture was purified with EZNA Gel Extraction Kit (Omega, USA). Then, sequencing libraries were generated using NEBNext® Ultra™ DNA Library Prep Kit for Illumina® (New England Biolabs, USA) following the manufacturer's recommendations and index codes were added. The library quality was assessed on the Qubit 2.0 Fluorometer (Thermo Scientific) and Agilent Bioanalyzer 2100 system. Lastly, the library was sequenced on an Illumina Hiseq 2500 platform and 250 bp paired-end reads were generated.

Sequencing data processing

Quality filtering on the paired-end raw reads was performed under specific filtering conditions to obtain the high-quality clean reads according to the Trimmomatic (V0.33, http://www.usadellab.org/cms/?page=trimmomatic) quality controlled process. Paired-end clean reads were merged using FLASH (V1.2.11, https://ccb.jhu.edu/software/FLASH/) according to the relationship of the

overlap between the paired-end reads, when at least 10 of the reads overlap the read generated from the opposite end of the same DNA fragment, the maximum allowable error ratio of the overlap region of 0.1, and the spliced sequences were called Raw Tags. Sequences were assigned to each sample based on their unique barcode and primer using Mothur software (V1.35.1, http://www.mothur.org), after which the barcodes and primers were removed and got the effective Clean Tags.

OTU cluster and Species annotation

Sequences analysis was performed by usearch software (V10, http://www.drive5.com/usearch/). Sequences with ≥97% similarity were assigned to the same OTU. An OTU is thought to possibly represent a species. The most frequently occurring sequence was extracted as a representative sequence for each OTU and was screened for further annotation.

LGG treatment

Mice were orally inoculated with LGG (ATCC 53103) (Bayer) (5×10^9 CFU per 200µl of saline) daily for 5 days according to the manufacturer's instructions. Briefly, the commercially obtained LGG was maintained in corn oil with a concentration of 5×10^9 CFU per 5 drops. Drops of LGG were diluted in saline for gavage and the same amount of corn oil (Sigma-Aldrich) drops without LGG was diluted in saline as a control.

Statistical analysis

All data were analyzed with GraphPad Prism 7.0 software. To calculate p-values, the unpaired two-tailed Student's t test was used for two-group datasets and one-way ANOVA was used for multi-group (more than two groups) datasets. Gehan-Breslow-Wilcoxon test was used for survival rate analysis. The specific data analysis is described in each figure legend.

Data availability

Raw illumina sequence data of the 16SrRNA gene generated in the study are available in the NCBI Sequence Read Archive(SRA) under accession number PRJNA579590.

Author contributions

DT and TZ performed and analyzed majority of all experiments, YW participated in most of the experiments, HC, JW, BZ, ZT, and LZ helped with sample collection, GBG gave suggestions and helped with writing of the manuscript. DT and ST conceived and designed the experiments. The manuscript was written by TZ, GBG, and ST and commented on by all other authors.

Disclosure of Potential Conflicts of Interest

No potential conflicts of interest were disclosed.

ORCID

Duozhuang Tang 🞅 http://orcid.org/0000-0002-7725-205X
Ting Zeng 🞅 http://orcid.org/0000-0002-4586-7869
Yiting Wang 🞅 http://orcid.org/0000-0001-8599-2165
Hui Cui 🞅 http://orcid.org/0000-0001-5255-322X
Jianying Wu 🞅 http://orcid.org/0000-0003-3691-1933
Bing Zou 🞅 http://orcid.org/0000-0001-9941-4796
Zhendong Tao 🞅 http://orcid.org/0000-0002-4188-8603
Liu Zhang 🞅 http://orcid.org/0000-0001-9923-260X
George B. Garside 🞅 http://orcid.org/0000-0002-8772-9616
Si Tao 🞅 http://orcid.org/0000-0001-6956-8516

References

1. Chan ES, Cronstein BN. Methotrexate–how does it really work? Nat Rev Rheumatol. 2010;6:175–178. PMID:20197777. doi:10.1038/nrrheum.2010.5.
2. Visentin M, Zhao R, Goldman ID. The antifolates. Hematol Oncol Clin North Am. 2012;26:629–48,ix. PMID:22520983. doi:10.1016/j.hoc.2012.02.002.
3. Bookbinder SA, Espinoza LR, Fenske NA, Germain BF, Vasey FB. Methotrexate: its use in the rheumatic diseases. Clin Exp Rheumatol. 1984;2:185–193. PMID:6398173.
4. Toffoli G, Russo A, Innocenti F, Corona G, Tumolo S, Sartor F, Mini E, Boiocchi M. Effect of methylenetetrahydrofolate reductase 677C–>T polymorphism on

toxicity and homocysteine plasma level after chronic methotrexate treatment of ovarian cancer patients. Int J Cancer. 2003;103:294–299. PMID:12471611. doi:10.1002/ijc.10847.

5. Brown PM, Pratt AG, Isaacs JD. Mechanism of action of methotrexate in rheumatoid arthritis, and the search for biomarkers. Nat Rev Rheumatol. 2016;12:731–742. PMID:27784891. doi:10.1038/nrrheum.2016.175.

6. Weinstein GD. Methotrexate. Ann Intern Med. 1977;86:199–204. PMID:319725. doi:10.7326/0003-4819-86-2-199.

7. Andersen JB, Szumlanski C, Weinshilboum RM, Schmiegelow K. Pharmacokinetics, dose adjustments, and 6-mercaptopurine/methotrexate drug interactions in two patients with thiopurine methyltransferase deficiency. Acta Paediatr (Oslo, Norway: 1992) 1998; 87:108–111; PMID:9510461. ;:. . doi:10.1080/08035259850158001.

8. Fotoohi AK, Albertioni F. Mechanisms of antifolate resistance and methotrexate efficacy in leukemia cells. Leuk Lymphoma. 2008;49:410–426. PMID:18297517. doi:10.1080/10428190701824569.

9. Freeman-Narrod M, Narrod SA. Chronic toxicity of methotrexate in mice. J Natl Cancer Inst. 1977;58:735–741. PMID:839565. doi:10.1093/jnci/58.3.735.

10. Aparicio-Domingo P, Romera-Hernandez M, Karrich JJ, Cornelissen F, Papazian N, Lindenbergh-Kortleve DJ, Butler JA, Boon L, Coles MC, Samsom JN, et al. Type 3 innate lymphoid cells maintain intestinal epithelial stem cells after tissue damage. J Exp Med. 2015;212:1783–1791. PMID:26392223. doi:10.1084/jem.20150318.

11. Neradil J, Pavlasova G, Veselska R. New mechanisms for an old drug; DHFR- and non-DHFR-mediated effects of methotrexate in cancer cells. Klin Onkol. 2012;25(Suppl 2):2s87–92. PMID:23581023.

12. de Koning BA, van Dieren JM, Lindenbergh-Kortleve DJ, van der Sluis M, Matsumoto T, Yamaguchi K, Einerhand AW, Samsom JN, Pieters R, Nieuwenhuis EE. Contributions of mucosal immune cells to methotrexate-induced mucositis. Int Immunol. 2006;18:941–949. PMID:16636014. doi:10.1093/intimm/dxl030.

13. Boukhettala N, Leblond J, Claeyssens S, Faure M, Le Pessot F, Bole-Feysot C, Hassan A, Mettraux C, Vuichoud J, Lavoinne A, et al. Methotrexate induces intestinal mucositis and alters gut protein metabolism independently of reduced food intake. Am J Physiol Endocrinol Metab. 2009;296:E182–90. PMID:18984853. doi:10.1152/ajpendo.90459.2008.

14. de Araujo AA, Borba PB, de Souza FH, Nogueira AC, Saldanha TS, Araujo TE, da Silva AI, de Araujo Junior RF. In a methotrexate-induced model of intestinal mucositis, olmesartan reduced inflammation and induced enteropathy characterized by severe diarrhea, weight loss, and reduced sucrose activity. Biol Pharm Bull. 2015;38:746–752. PMID:25947920. doi:10.1248/bpb.b14-00847.

15. Elting LS, Cooksley C, Chambers M, Cantor SB, Manzullo E, Rubenstein EB. The burdens of cancer therapy. Clinical and economic outcomes of chemotherapy-induced mucositis. Cancer. 2003;98:1531–1539. PMID:14508842. doi:10.1002/cncr.11671.

16. Lee YS, Kim TY, Kim Y, Lee SH, Kim S, Kang SW, Yang JY, Baek IJ, Sung YH, Park YY, et al. Microbiota-derived lactate accelerates intestinal stem-cell-mediated epithelial development. Cell Host Microbe. 2018;24:833–46.e6. PMID:30543778. doi:10.1016/j.chom.2018.11.002.

17. Tinkum KL, Stemler KM, White LS, Loza AJ, Jeter-Jones S, Michalski BM, Kuzmicki C, Pless R, Stappenbeck TS, Piwnica-Worms D, et al. Fasting protects mice from lethal DNA damage by promoting small intestinal epithelial stem cell survival. Proc Natl Acad Sci USA. 2015;112:E7148–54. PMID:26644583. doi:10.1073/pnas.1509249112.

18. Barker N, Clevers H. Tracking down the stem cells of the intestine: strategies to identify adult stem cells. Gastroenterology. 2007;133:1755–1760. PMID:18054544. doi:10.1053/j.gastro.2007.10.029.

19. Ritsma L, Ellenbroek SIJ, Zomer A, Snippert HJ, de Sauvage FJ, Simons BD, Clevers H, van Rheenen J. Intestinal crypt homeostasis revealed at single-stem-cell level by in vivo live imaging. Nature. 2014;507:362–365. PMID:24531760. doi:10.1038/nature12972.

20. Potten CS, Al-Barwari SE, Searle J. Differential radiation response amongst proliferating epithelial cells. Cell Tissue Kinet. 1978;11:149–160. PMID:630578. doi:10.1111/j.1365-2184.1978.tb00883.x.

21. Gregorieff A, Liu Y, Inanlou MR, Khomchuk Y, Wrana JL. Yap-dependent reprogramming of Lgr5(+) stem cells drives intestinal regeneration and cancer. Nature. 2015;526:715–718. PMID:26503053. doi:10.1038/nature15382.

22. Ayyaz A, Kumar S, Sangiorgi B, Ghoshal B, Gosio J, Ouladan S, Fink M, Barutcu S, Trcka D, Shen J, et al. Single-cell transcriptomes of the regenerating intestine reveal a revival stem cell. Nature. 2019;569:121–125. PMID:31019301. doi:10.1038/s41586-019-1154-y.

23. Metcalfe C, Kljavin NM, Ybarra R, de Sauvage FJ. Lgr5+ stem cells are indispensable for radiation-induced intestinal regeneration. Cell Stem Cell. 2014;14:149–159. PMID:24332836. doi:10.1016/j.stem.2013.11.008.

24. Tao S, Tang D, Morita Y, Sperka T, Omrani O, Lechel A, Sakk V, Kraus J, Kestler HA, Kuhl M, et al. Wnt activity and basal niche position sensitize intestinal stem and progenitor cells to DNA damage. Embo J. 2015;34:624–640. PMID:25609789. doi:10.15252/embj.201490700.

25. Zhou B, Xia X, Wang P, Chen S, Yu C, Huang R, Zhang R, Wang Y, Lu L, Yuan F, et al. Induction and amelioration of methotrexate-induced gastrointestinal toxicity are related to immune response and gut microbiota. EBioMedicine. 2018;33:122–133. PMID:30049384. doi:10.1016/j.ebiom.2018.06.029.

26. Liu T, Wu Y, Wang L, Pang X, Zhao L, Yuan H, Zhang C. A more robust gut microbiota in calorie-restricted mice is associated with attenuated intestinal injury caused by the chemotherapy drug cyclophosphamide. mBio. 2019;10. PMID:30862756. doi:10.1128/mBio.02903-18.

27. Tang D, Tao S, Chen Z, Koliesnik IO, Calmes PG, Hoerr V, Han B, Gebert N, Zornig M, Loffler B, et al. Dietary restriction improves repopulation but impairs lymphoid differentiation capacity of hematopoietic stem cells in early aging. J Exp Med. 2016;213:535–553. PMID:26951333. doi:10.1084/jem.20151100.

28. Cerletti M, Jang YC, Finley LW, Haigis MC, Wagers AJ. Short-term calorie restriction enhances skeletal muscle stem cell function. Cell Stem Cell. 2012;10:515–519. PMID:22560075. doi:10.1016/j.stem.2012.04.002.

29. Begus-Nahrmann Y, Lechel A, Obenauf AC, Nalapareddy K, Peit E, Hoffmann E, Schlaudraff F, Liss B, Schirmacher P, Kestler H, et al. p53 deletion impairs clearance of chromosomal-instable stem cells in aging telomere-dysfunctional mice. Nat Genet. 2009;41:1138–1143. PMID:19718028. doi:10.1038/ng.426.

30. Sato T, Vries RG, Snippert HJ, van de Wetering M, Barker N, Stange DE, van Es JH, Abo A, Kujala P, Peters PJ, et al. Single Lgr5 stem cells build crypt-villus structures in vitro without a mesenchymal niche. Nature. 2009;459:262–265. PMID:19329995. doi:10.1038/nature07935.

31. Starr ME, Steele AM, Cohen DA, Saito H. Short-term dietary restriction rescues mice from lethal abdominal sepsis and endotoxemia and reduces the inflammatory/coagulant potential of adipose tissue. Crit Care Med. 2016;44:e509–19. PMID:26646465. doi:10.1097/ccm.0000000000001475.

32. Apple DM, Mahesula S, Fonseca RS, Zhu C, Kokovay E. Calorie restriction protects neural stem cells from age-related deficits in the subventricular zone. Aging. 2019;11:115–126. PMID:30622221. doi:10.18632/aging.101731.

33. Mao Y, Nobaek S, Kasravi B, Adawi D, Stenram U, Molin G, Jeppsson B. The effects of Lactobacillus strains and oat fiber on methotrexate-induced enterocolitis in rats. Gastroenterology. 1996;111:334–344. PMID:8690198. doi:10.1053/gast.1996.v111.pm8690198.

34. Wei D, Heus P, van de Wetering FT, van Tienhoven G, Verleye L, Scholten RJ. Probiotics for the prevention or treatment of chemotherapy- or radiotherapy-related diarrhoea in people with cancer. Cochrane Database Syst Rev. 2018;8:Cd008831. PMID:30168576. doi:10.1002/14651858.CD008831.pub3.

35. Ciorba MA, Riehl TE, Rao MS, Moon C, Ee X, Nava GM, Walker MR, Marinshaw JM, Stappenbeck TS, Stenson WF. Lactobacillus probiotic protects intestinal epithelium from radiation injury in a TLR-2/cyclo-oxygenase-2-dependent manner. Gut. 2012;61:829–838. PMID:22027478. doi:10.1136/gutjnl-2011-300367.

36. Riehl TE, Alvarado D, Ee X, Zuckerman A, Foster L, Kapoor V, Thotala D, Ciorba MA, Stenson WF. Lactobacillus rhamnosus GG protects the intestinal epithelium from radiation injury through release of lipoteichoic acid, macrophage activation and the migration of mesenchymal stem cells. Gut. 2018. PMID:29934438. doi: 10.1136/gutjnl-2018-316226.

37. Longo VD, Fontana L. Calorie restriction and cancer prevention: metabolic and molecular mechanisms. Trends Pharmacol Sci. 2010;31:89–98. PMID:20097433. doi:10.1016/j.tips.2009.11.004.

38. Meynet O, Zunino B, Happo L, Pradelli LA, Chiche J, Jacquin MA, Mondragon L, Tanti JF, Taillan B, Garnier G, et al. Caloric restriction modulates Mcl-1 expression and sensitizes lymphomas to BH3 mimetic in mice. Blood. 2013;122:2402–2411. PMID:23966420. doi:10.1182/blood-2013-01-478651.

39. Shelton LM, Huysentruyt LC, Mukherjee P, Seyfried TN. Calorie restriction as an anti-invasive therapy for malignant brain cancer in the VM mouse. ASN Neuro. 2010;2:e00038. PMID:20664705. doi:10.1042/an20100002.

40. Lee C, Raffaghello L, Brandhorst S, Safdie FM, Bianchi G, Martin-Montalvo A, Pistoia V, Wei M, Hwang S, Merlino A, et al. Fasting cycles retard growth of tumors and sensitize a range of cancer cell types to chemotherapy. Sci Transl Med. 2012;4:124ra27. PMID:22323820. doi:10.1126/scitranslmed.3003293.

41. Meynet O, Ricci JE. Caloric restriction and cancer: molecular mechanisms and clinical implications. Trends Mol Med. 2014;20:419–427. PMID:24916302. doi:10.1016/j.molmed.2014.05.001.

42. Nguyen TL, Vieira-Silva S, Liston A, Raes J. How informative is the mouse for human gut microbiota research? Dis Model Mech. 2015;8:1–16. PMID:25561744. doi:10.1242/dmm.017400.

43. Hugenholtz F, de Vos WM. Mouse models for human intestinal microbiota research: a critical evaluation. Cell Mol Life Sci. 2018;75:149–160. PMID:29124307. doi:10.1007/s00018-017-2693-8.

44. Haro C, Rangel-Zuniga OA, Alcala-Diaz JF, Gomez-Delgado F, Perez-Martinez P, Delgado-Lista J, Quintana-Navarro GM, Landa BB, Navas-Cortes JA, Tena-Sempere M, et al. Intestinal microbiota is influenced by gender and body mass index. PLoS One. 2016;11:e0154090. PMID:27228093. doi:10.1371/journal.pone.0154090.

45. Markle JG, Frank DN, Mortin-Toth S, Robertson CE, Feazel LM, Rolle-Kampczyk U, von Bergen M, McCoy KD, Macpherson AJ, Danska JS. Sex differences in the gut microbiome drive hormone-dependent regulation of autoimmunity. Science. 2013;339:1084–1088. PMID:23328391. doi:10.1126/science.1233521.

46. Yurkovetskiy L, Burrows M, Khan AA, Graham L, Volchkov P, Becker L, Antonopoulos D, Umesaki Y, Chervonsky AV. Gender bias in autoimmunity is

influenced by microbiota. Immunity. 2013;39:400–412. PMID:23973225. doi:10.1016/j.immuni.2013.08.013.

47. Xiao L, Feng Q, Liang S, Sonne SB, Xia Z, Qiu X, Li X, Long H, Zhang J, Zhang D, et al. A catalog of the mouse gut metagenome. Nat Biotechnol. 2015;33:1103–1108. PMID:26414350. doi:10.1038/nbt.3353.

48. Touchefeu Y, Montassier E, Nieman K, Gastinne T, Potel G, Bruley Des Varannes S, Le Vacon F, de La Cochetiere MF. Systematic review: the role of the gut microbiota in chemotherapy- or radiation-induced gastro-intestinal mucositis - current evidence and potential clin-ical applications. Aliment Pharmacol Ther. 2014;40:409–421. PMID:25040088. doi:10.1111/apt.12878.

49. Hagan T, Cortese M, Rouphael N, Boudreau C, Linde C, Maddur MS, Das J, Wang H, Guthmiller J, Zheng NY, et al. Antibiotics-driven gut microbiome perturbation alters immunity to vaccines in humans. Cell. 2019;178:1313–28.e13. PMID:31491384. doi:10.1016/j.cell.2019.08.010.

50. Alexander JL, Wilson ID, Teare J, Marchesi JR, Nicholson JK, Kinross JM. Gut microbiota modulation of chemotherapy efficacy and toxicity. Nat Rev Gastro Hepat. 2017;14:356–365. PMID:28270698. doi:10.1038/nrgastro.2017.20.

51. Jordan KR, Loman BR, Bailey MT, Pyter LM. Gut microbiota-immune-brain interactions in chemo therapy-associated behavioral comorbidities. Cancer. 2018;124:3990–3999. PMID:29975400. doi:10.1002/cncr.31584.

52. Burrello C, Garavaglia F, Cribiu FM, Ercoli G, Lopez G, Troisi J, Colucci A, Guglietta S, Carloni S, Guglielmetti S, et al. Therapeutic faecal microbiota transplantation con-trols intestinal inflammation through IL10 secretion by immune cells. Nat Commun. 2018;9:5184. PMID: 30518790. doi:10.1038/s41467-018-07359-8.

53. Postler TS, Ghosh S. Understanding the holobiont: how microbial metabolites affect human health and shape the immune system. Cell Metab. 2017;26:110–130. PMID:28625867. doi:10.1016/j.cmet.2017.05.008.

54. Thomsen M, Clarke S, Vitetta L. The role of adjuvant probiotics to attenuate intestinal inflammatory responses due to cancer treatments. Benef Microbes. 2018;9:899–916. PMID:30232908. doi:10.3920/bm2017.0172.

55. Prisciandaro LD, Geier MS, Butler RN, Cummins AG, Howarth GS. Evidence supporting the use of probio-tics for the prevention and treatment of chemotherapy-induced intestinal mucositis. Crit Rev Food Sci Nutr. 2011;51:239–247. PMID:21390944. doi:10.1080/10408390903551747.

56. Scheinberg P, Townsley D, Dumitriu B, Scheinberg P, Weinstein B, Daphtary M, Rios O, Wu CO, Young NS. Moderate-dose cyclophosphamide for severe aplastic anemia has significant toxicity and does not prevent relapse and clonal evolution. Blood. 2014;124:2820–2823. PMID:25185712. doi:10.1182/blood-2014-05-573642.

57. Shepherd JD, Pringle LE, Barnett MJ, Klingemann HG, Reece DE, Phillips GL. Mesna versus hyperhydration for the prevention of cyclophosphamide-induced hemorrhagic cystitis in bone marrow transplantation. J Clin Oncol. 1991;9:2016–2020. PMID:1941060. doi:10.1200/jco.1991.9.11.2016.

58. Miser JS, Kinsella TJ, Triche TJ, Tsokos M, Jarosinski P, Forquer R, Wesley R, Magrath I. Ifosfamide with mesna uroprotection and etopo-side: an effective regimen in the treatment of recur-rent sarcomas and other tumors of children and young adults. J Clin Oncol. 1987;5:1191–1198. PMID:3114435. doi:10.1200/jco.1987.5.8.1191.

59. Karlsson MO, Port RE, Ratain MJ, Sheiner LB. A population model for the leukopenic effect of etoposide. Clin Pharmacol Ther. 1995;57:325–334. PMID:7697950. doi:10.1016/0009-9236(95)90158-2.

60. Sonis ST, Elting LS, Keefe D, Peterson DE, Schubert M, Hauer-Jensen M, Bekele BN, Raber-Durlacher J, Donnelly JP, Rubenstein EB. Perspectives on cancer therapy-induced mucosal injury: pathogenesis, measure-ment, epidemiology, and consequences for patients. Cancer. 2004;100:1995–2025. PMID:15108222. doi:10.1002/cncr.20162.

61. Rudolph KL, Millard M, Bosenberg MW, DePinho RA. Telomere dysfunction and evolution of intestinal car-cinoma in mice and humans. Nat Genet. 2001;28:155–159. PMID:11381263. doi:10.1038/88871.

62. Cui H, Tang D, Garside GB, Zeng T, Wang Y, Tao Z, Zhang L, Tao S. Wnt signaling mediates the aging-induced differentiation impairment of intestinal stem cells. Stem Cell Rev. 2019;15:448–455. PMID:30790135. doi:10.1007/s12015-019-09880-9.

63. Seo SU, Kamada N, Munoz-Planillo R, Kim YG, Kim D, Koizumi Y, Hasegawa M, Himpsl SD, Browne HP, Lawley TD, et al. Distinct commensals induce interleukin-1beta via NLRP3 inflammasome in inflamma-tory monocytes to promote intestinal inflammation in response to injury. Immunity. 2015;42:744–755. PMID:25862092. doi:10.1016/j.immuni.2015.03.004.

64. Bamias G, Martin C, Mishina M, Ross WG, Rivera-Nieves J, Marini M, Cominelli F. Proinflammatory effects of TH2 cytokines in a murine model of chronic small intestinal inflammation. Gastroenterology. 2005;128:654–666. PMID:15765401. doi:10.1053/j.gastro.2004.11.053.

65. Sassone-Corsi M, Nuccio SP, Liu H, Hernandez D, Vu CT, Takahashi AA, Edwards RA, Raffatellu M. Microcins med-iate competition among Enterobacteriaceae in the inflamed gut. Nature. 2016;540:280–283. PMID:27798599. doi:10.1038/nature20557.

66. Zhang R, Daroczy K, Xiao B, Yu L, Chen R, Liao Q. Qualitative and semiquantitative analysis of Lactobacillus species in the vaginas of healthy fertile and postmenopausal Chinese women. J Med Microbiol. 2012;61:729–739. PMID:22301614. doi:10.1099/jmm.0.038687-0.

67. Hayashi A, Mikami Y, Miyamoto K, Kamada N, Sato T, Mizuno S, Naganuma M, Teratani T, Aoki R, Fukuda S, et al. Intestinal dysbiosis and biotin deprivation induce alopecia through overgrowth of Lactobacillus murinus in mice. Cell Rep. 2017;20:1513–1524. PMID:28813664. doi:10.1016/j.celrep.2017.07.057.

68. Turner S, Pryer KM, Miao VP, Palmer JD. Investigating deep phylogenetic relationships among cyanobacteria and plastids by small subunit rRNA sequence analysis. J Eukaryot Microbiol. 1999; 46:327–338. PMID:10461381. doi:10.1111/j.1550-7408.1999.tb04612.x.

69. DJ Lane. 16S/23S rRNA sequencing. In Stackebrandt E, Goodfellow M, editors. Nucleic acid techniques in bacterial systematics. New York: John Wiley & Sons; 1991. p. 115–175.

70. Huws SA, Edwards JE, Kim EJ, Scollan ND. Specificity and sensitivity of eubacterial primers utilized for molecular profiling of bacteria within complex microbial ecosystems. J Microbiol Methods. 2007;70:565–569. PMID:17683816. doi:10.1016/j.mimet.2007.06.013.